CCD PHOTOMETRY OF THE OPEN CLUSTERS NGC 2671 AND ANONYMOUS HAFFNER 17 (C0749–317)

M. H. Pedreros[1]

Departamento de Física, Fac. de Ciencias
Universidad de Tarapacá, Arica, Chile

RESUMEN

Se presenta un estudio fotométrico UBV preliminar, basado en nuevas observaciones CCD, para la región central de los cúmulos abiertos NGC 2671 y Anonymous Haffner 17 (C0749–317). Usando un programa computacional que ajusta la sequencia principal de la edad cero a los datos del cúmulo, se determinaron los enrojecimientos y módulos de distancia medios para los dos cúmulos dando los valores $E_{B-V}(B0V) = 1.04 \pm 0.02$ (s.d.) y $V_0 - M_V = 11.1 \pm 0.5$ (s.d) para NGC 2671, y $E_{B-V}(B0V) = 1.26 \pm 0.04$ (s.d.) y $V_0 - M_V = 12.3 \pm 0.2$ (s.d.) para C0749–317. Se hizo una estimación de la edad de los cúmulos obteniendo 8×10^7 años y 5×10^7 años para NGC 2671 y C0749–317, respectivamente. El último cúmulo parece localizarse cerca de la continuación de nuestro brazo espiral local.

ABSTRACT

A preliminary UBV photometric study, based upon new CCD observations, is presented for the central region of the open clusters NGC 2671 and Anonymous Haffner 17 (C0749–317). Using a zero-age main sequence fitting computer package, the average reddenings and distance moduli for the two clusters were determined yielding $E_{B-V}(B0V) = 1.04 \pm 0.02$ (s.d.) and $V_0 - M_V = 11.1 \pm 0.5$ (s.d) for NGC 2671 and $E_{B-V}(B0V) = 1.26 \pm 0.04$ (s.d.), and $V_0 - M_V = 12.3 \pm 0.2$ (s.d.) for C0749–317. An estimate of the clusters age was also made resulting in values of 8×10^7 yrs and 5×10^7 yrs, for NGC 2671 and C0749–317, respectively. The latter cluster seems to locate near the continuation of our local spiral arm feature.

Key words: **OPEN CLUSTERS AND ASSOCIATIONS: INDIVIDUAL: NGC 2671, HAFFNER 17 (C0749–317) — TECHNIQUES: PHOTOMETRIC**

1. INTRODUCTION

The open cluster NGC 2671 ($\alpha_{1950} = 08^h\ 44.4^m$, $\delta_{1950} = -41°\ 42'$; $l = 262°.15$, $b = +0°.79$) has been classified as a Trumpler class I 3 p cluster (Ruprecht 1966), i.e., a relatively poor, detached cluster with stars in a wide range of brightness and a strong central concentration. The open cluster C0749–317 ($\alpha_{1950} = 07^h\ 49.8^m$, $\delta_{1950} = -31°43'$; $l = 247°.72$, $b = -2°.53$); on the other hand, has been classed as

a Trumpler class III 3 p cluster (Ruprecht 1966), i.e., showing the same morphological properties described above with the exception of the strong central concentration. Neither cluster has previous standardized photometric observations reported. Nevertheless, NGC 2671 has been part of a search program (Phelps, Janes, & Montgomery 1994) for old open clusters where only instrumental CCD photometry is presented.

This study is part of a project, started in December 1985, aimed to systematically observe all those CCD observable open clusters (specially those with small angular diameter) that had not been studied or with insufficient and/or bad quality photometry at the time this program was initiated. One of these clusters (C0749–317) is located within the 200–260

---

range in Galactic longitude which is believed to be relatively free from nearby dust clouds (FitzGerald 1968; Lucke 1978) allowing, in this way, for long distance observations, the other cluster locates close to this range. The interest in observing distant clusters resides in that their metallicities and/or luminosity functions may differ from what we know for the solar neighborhood (Cameron 1985). In addition to this, if some of the clusters in this program turn out to be young, they may be used in the study of the structure of the spiral features of the Galaxy, where we could compare our results with those based on radio observations made within this longitude range.

This paper presents UBV CCD observations in the area of NGC 2671 and C0749–317 extending down to a limiting magnitude of $V < 17$, from which we will obtain preliminary values of reddenings, distance moduli and ages for the two clusters.

2. OBSERVATIONS AND REDUCTIONS

The observations reported here, were obtained at Cerro Tololo Inter American Observatory with the RCA CCD camera attached to the 0.9-m telescope during the night of December 12/13 (C0749–317) and December 14/15 (NGC 2671), 1985, as part of an observing run extending from December 11/12 to December 15/16. The image scale was 0.495 arcsec/pixel (pixel size = 30 × 30 μm), corresponding to a field of 2.6 × 4.2 arcmin for the 320 × 512 pixel

TABLE 1

CERRO TOLOLO CCD OBSERVATIONS

Cluster	Frame	Filter	Exposure Time (s)
NGC 2671	241	B	20
	242	B	20
	243	B	20
	244	V	15
	245	V	15
	246	V	15
	247	U	240
Haff 17	067	B	120
	068	B	120
	069	V	90
	070	V	90
	077	U	600

field. The program frames consisted of a set of UBV exposures of the open clusters NGC 2671 and C0749–317 central region. The filters used correspond to U, B, V CCD filters available at the dome at the time of observation. The acquisition and preprocess-
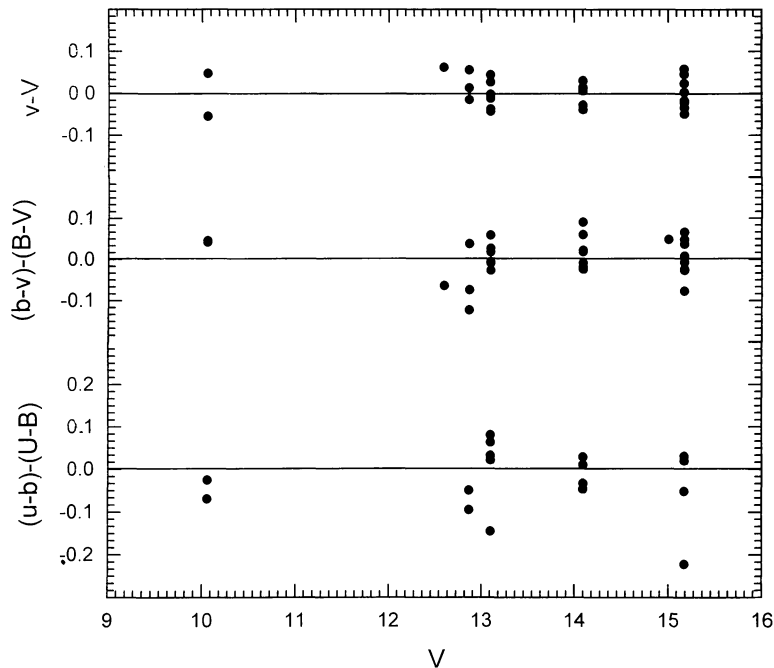

Fig. 1. Adopted *minus* standard photometry residuals versus V magnitude for standard stars. V, $B - V$, and $U - B$ represent standard values whereas v, $b - v$, and $u - b$ stand for their CCD adopted counterparts obtained after running the instrumental magnitudes through the transformation equations.

PEDREROS

Fig. 3. Finding chart for the stars in the central region of C0749–317 listed in Table 3 and reproduced from the V working frame obtained from the average of two 90 s exposure frames. The orientation and size are as in Figure 1.
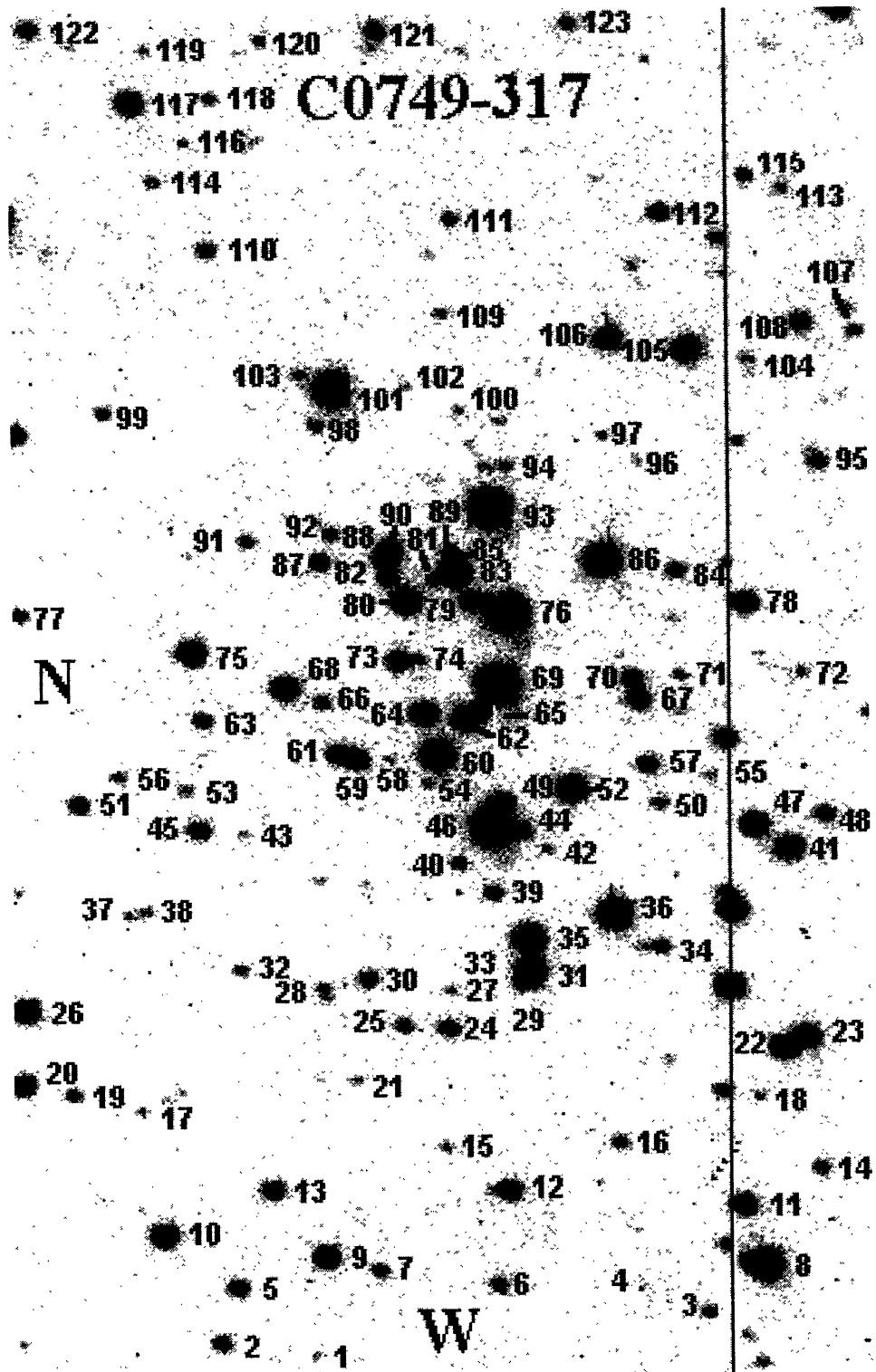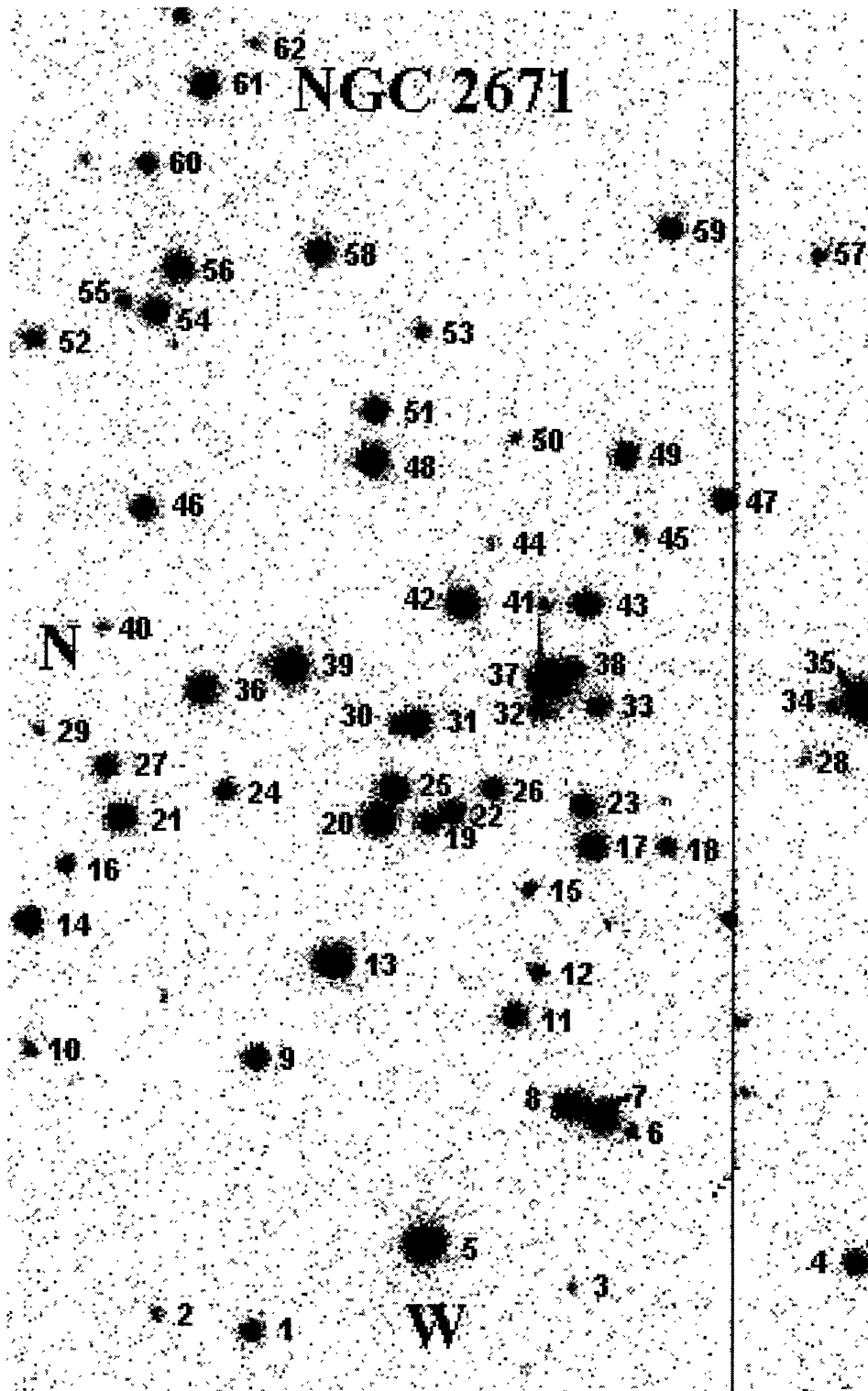
Fig. 2. Finding chart for the stars in the central region of NGC 2671 listed in Table 2 and reproduced from the *V* working frame obtained from the average of three 15 s exposure frames. The entire 2.6 × 4.2 arcmin field is shown wherein north is at the left and east at the top of the picture.

ing of the program frames was carried out using the Cassegrain Focus CCD system acquisition and reduction software available through TOLNET link at the 0.9-m telescope dome at the time of the observations. Table 1 shows the list of individual frames obtained for each filter. A single working frame *per* passband was obtained by averaging individual frames of the same passband. The final reduction of the data was made through IRAF digital photometry routines, mainly DAOPHOT (Stetson 1987). A total of seven UBV standard stars in the E-regions (Graham 1982) were observed during the entire run, between the dates given above, at an average of three different hour angles *per* night *per* star, so as to obtain the coefficients to transform the instrumental magnitudes to the standard system defined by these stars. The adopted transformation equations were of the form: $m_{inst} = m_{std} + c_1 + c_2 X + c_3(CI)$, where c_1, c_2, c_3 are the transformation coeficients, X is the airmass and CI is the color index, which corresponds to $U - B$, $B - V$, and $B - V$ for m_{std} equal to U, B, and V, respectively. The standard deviations of the corresponding fits to the transformation equations given above were: $\pm$ 0.08, $\pm$ 0.03, and $\pm$ 0.03 for U, B, and V, respectively. Figure 1 shows the residuals (adopted *minus* standard) for the standard star photometry as a function of the standard V magnitude. The adopted photometry resulted from

TABLE 2

CCD PHOTOMETRY FOR STARS IN THE CENTRAL REGION
OF NGC 2671

Star (1)	V (2)	$U - B$ (3)	$B - V$ (4)	Rem (5)	Star (1)	V (2)	$U - B$ (3)	$B - V$ (4)	Rem (5)
1	15.75	...	1.07		32	17.02	...	0.02	
2	17.29	...	0.99		33	15.71	...	1.00	
3	17.55	...	1.35		34	17.35	...	0.99	
4	15.13	0.62	0.96	M	35	12.82	-0.13	0.48	
5	13.00	0.34	0.88		36	14.15	0.42	1.08	
6	17.24	...	1.22		37	12.90	-0.07	0.69	
7	14.01	0.40	0.89	M	38	15.67	...	0.90	
8	14.19	0.30	0.87	M	39	13.31	...	1.99	
9	15.11	0.40	1.05		40	17.40	...	1.29	
10	16.61	...	1.26		41	17.33	...	0.71	
11	15.02	0.42	0.95	M	42	14.00	0.33	0.97	M
12	16.49	...	1.32		43	14.67	0.20	1.04	
13	13.36	0.33	0.99	M	44	17.76	...	0.67	
14	14.51	...	1.89		45	17.16	...	1.37	
15	16.60	...	2.20		46	15.14	0.23	1.03	
16	16.34	...	1.21		47	15.25	...	0.90	
17	14.51	0.34	0.91	M	48	14.11	0.48	0.90	M
18	16.17	...	1.06		49	14.91	0.32	0.99	M
19	15.40	0.52	1.10		50	17.36	...	1.25	
20	13.77	0.29	0.96	M	51	14.92	0.55	0.95	M
21	14.25	0.41	1.06		52	15.92	...	1.25	
22	15.11	0.23	0.93	M	53	16.45	...	1.74	
23	14.81	0.46	0.97	M	54	14.58	0.51	1.03	M
24	15.64	...	1.15		55	16.79	...	1.37	
25	14.38	0.48	1.11		56	14.34	...	2.23	
26	15.30	0.45	0.94	M	57	16.54	...	1.40	
27	15.33	0.48	1.07		58	14.72	0.57	0.85	
28	17.60	...	0.94		59	15.11	0.44	1.03	M
29	17.44	...	1.35		60	15.79	...	1.24	
30	15.92	...	1.00		61	14.56	0.44	0.85	
31	14.51	0.41	0.93	M	62	17.46	...	1.55	

running the CCD instrumental photometry through the above transformation equations.

The resulting CCD photometry of the program stars identified in Figures 2 and 3 is listed in Tables 2 and 3, both with the same format. Column 1 shows the star identification as in Figs. 2 and 3. Columns 2 through 4 list the adopted CCD magnitude and colors obtained from running the instrumental magnitudes through the adopted transformation equations derived from the observations of E-regions standard stars. Column 5 indicates (with an M) the probable cluster members selected by the fitting program from stars with observed $U - B$ color, as explained in the next section.

In order to estimate the uncertainty of our results, we averaged the color and magnitude standard deviations of individual stars rendered by the IRAF NOAO transformation routines. The average

standard deviations obtained for program stars in NGC 2671 were: $\pm$ 0.018, $\pm$ 0.083, and $\pm$ 0.034 for V, $U - B$, and $B - V$, respectively, for stars with $V \leq 16$, and $\pm$ 0.052 and $\pm$ 0.123 for V and $B - V$, respectively, for stars in the range $16 < V < 17$. In the same way, the averages we obtained for stars in C0749–317 were: $\pm$ 0.008, $\pm$ 0.068, and $\pm$ 0.017 for V, $U - B$, and $B - V$, respectively, for stars with $V \leq 16$, and $\pm$ 0.014, $\pm$ 0.130, and $\pm$ 0.030 for V, $U - B$, and $B - V$, respectively, for stars in the range $16 < V < 17$.

3. CLUSTER PARAMETER DETERMINATIONS

The individual color excesses and distance moduli for program stars with $U - B$ color available were obtained through a zero-age main sequence fitting computer package, written by the author and de-

TABLE 3

CCD PHOTOMETRY FOR STARS IN THE CENTRAL REGION
OF C0749–317

Star (1)	V (2)	$U - B$ (3)	$B - V$ (4)	Rem (5)	Star (1)	V (2)	$U - B$ (3)	$B - V$ (4)	Rem (5)
1	19.35	...	1.65		63	17.60	...	1.44	
2	17.45	...	1.23		64	16.01	0.32	1.09	M
3	18.07	...	1.47		65	17.43	...	1.36	
4	19.68	...	1.27		66	17.93	...	1.69	
5	17.34	...	1.24		67	16.74	...	1.27	
6	17.95	...	1.32		68	15.82	...	1.10	
7	17.95	...	1.34		69	13.64	...	2.33	M?
8	14.67	0.68	1.43		70	17.02	...	1.34	
9	16.08	...	1.16		71	18.53	...	1.40	
10	15.94	0.40	1.06	M	72	18.54	...	2.20	
11	16.10	...	1.43		73	16.53	...	1.13	
12	16.64	...	1.20		74	18.87	...	1.63	
13	16.86	...	1.11		75	15.52	0.60	1.34	
14	18.11	...	1.59		76	13.62	...	2.29	M?
15	18.82	...	1.51		77	17.91	...	1.37	
16	18.16	...	1.42		78	16.13	...	1.29	
17	19.01	...	1.61		79	16.88	...	1.14	
18	19.02	...	2.43		80	15.53	0.23	1.06	M
19	17.98	...	1.22		81	18.45	...	1.44	
20	16.19	0.31	1.21		82	17.19	...	1.22	
21	19.02	...	1.28		83	15.48	0.47	1.13	M
22	15.86	...	1.42		84	17.51	...	1.38	
23	16.08	...	1.40		85	18.07	...	1.20	
24	17.21	...	1.04		86	14.54	0.46	1.17	
25	17.65	...	1.23		87	17.16	...	1.29	
26	15.92	0.35	1.11	M	88	16.17	0.33	1.11	M
27	18.91	...	1.95		89	17.38	...	1.29	
28	18.37	...	1.46		90	16.90	...	1.30	

TABLE 3 (CONTINUED)

Star (1)	V (2)	$U-B$ (3)	$B-V$ (4)	Rem (5)	Star (1)	V (2)	$U-B$ (3)	$B-V$ (4)	Rem (5)
29	18.56	...	1.66		91	18.16	...	1.26	
30	17.28	...	1.25		92	17.96	...	1.24	
31	15.36	0.25	1.02	M	93	13.82	0.34	1.11	
32	18.32	...	1.57		94	18.41	...	1.69	
33	18.74	...	1.92		95	17.71	...	1.18	
34	17.74	...	1.55		96	19.44	...	1.64	
35	15.19	0.37	1.08	M	97	18.80	...	1.41	
36	14.85	0.22	1.11		98	18.05	...	1.42	
37	18.98	...	1.30		99	18.16	...	1.55	
38	18.66	...	1.58		100	19.08	...	1.33	
39	17.70	...	1.37		101	14.31	0.17	0.71	
40	17.89	...	1.25		102	19.33	...	1.37	
41	15.94	...	1.27		103	18.58	...	1.22	
42	18.95	...	1.65		104	18.69	...	1.86	
43	19.31	...	1.98		105	15.52	...	1.17	
44	17.19	...	1.23		106	16.01	0.25	1.19	
45	16.98	...	1.35		107	18.31	...	1.43	
46	13.85	0.22	1.06		108	16.86	...	1.27	
47	15.74	0.58	1.23		109	18.63	...	1.27	
48	17.43	...	1.45		110	17.48	...	1.40	
49	16.60	...	1.25		111	18.02	...	1.43	
50	18.49	...	1.65		112	16.96	...	2.53	
51	17.20	...	1.28		113	18.70	...	1.45	
52	15.37	0.34	1.18		114	18.22	...	1.89	
53	18.76	...	1.26		115	17.89	...	1.58	
54	18.94	...	1.95		116	18.97	...	1.26	
55	19.09	...	1.82		117	15.64	...	2.77	
56	18.48	...	1.51		118	18.30	...	1.50	
57	17.08	...	1.25		119	19.18	...	1.47	
58	19.25	...	1.87		120	18.61	...	1.42	
59	16.57	...	1.15		121	17.19	...	1.33	
60	14.85	0.22	1.04		122	17.11	...	2.27	
61	16.84	...	1.30		123	17.94	...	1.30	

scribed elsewhere (Pedreros 1984), which automatically traces each star back to the adopted intrinsic color-color curve (ICCC) along their corresponding curved reddening lines, through successive iterations. Next, the package obtains the absolute magnitudes (M_V), by interpolating from the adopted Zero-Age Main Sequence (ZAMS), using the star's derived intrinsic $B-V$ color. For stars of spectral types earlier than A0 we adopted the ZAMS by Mermilliod (1981) and a combination of Heintze's (1973) and Mermilliod's (1981) ICCC. For spectral types later than A0, the adopted intrinsic curves are the ZAMS by Turner (1979) and a compromise between the ICCC

derived by Mermilliod (1981) and that by Schmidt-Kaler (1982). The adopted expressions for the curvatures of the reddening and the total-to-selective absorption ratio lines, are based on those given by Buser (1978). Initial values of $E_{U-B}/E_{B-V} = 0.72$ and $R = A/E_{B-V} = 3.1$, respectively, were adopted for the iteration process. The computed individual color excesses are then transformed into their equivalent for a B0V star and, as explained below, averaged over the sample of selected probable cluster members (those indicated with an M in column 5 of Tables 2 and 3) along with their distance moduli.
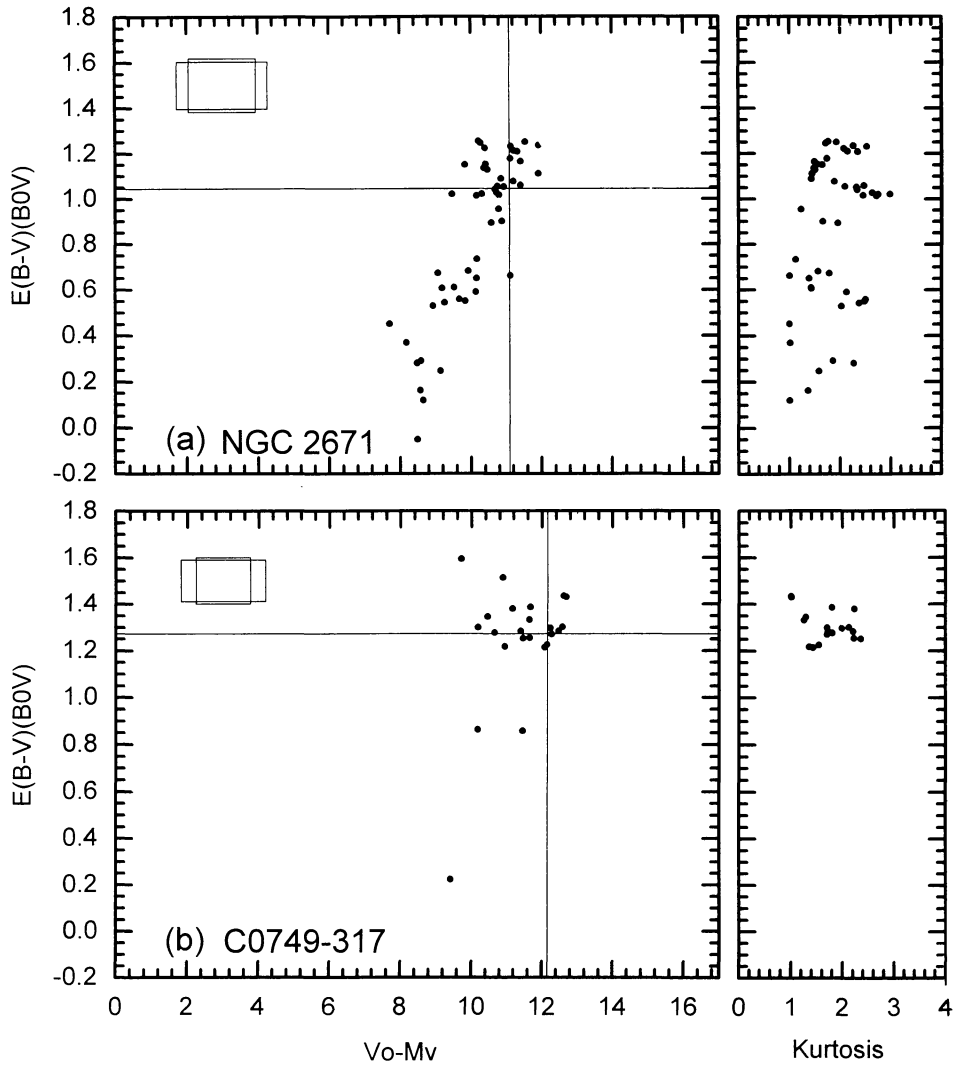
Figures 4 and 5 show the distance modulus-color

Fig. 4. Individual color excess versus individual distance modulus and kurtosis diagrams for NGC 2671 (*a*) and C0749–317 (*b*) resulting from the ZAMS fitting package. The adopted average color excess and distance modulus point is indicated by the crossing lines. An individual star could be represented by more than one point in the diagram depending on how many times its reddening line intersects the ICCC. The two rectangles on the upper left corner represent the search (the smaller one) and selecting (the larger one) error boxes. The maximum kurtosis value indicates the maximum concentration of data points within the search box.

excess and color-magnitude diagrams that resulted from running the stars in Tables 2 and 3 through the ZAMS fitting computer package. Figures 4(*a*) and (*b*) show the individual color excess versus individual distance modulus diagrams of the data that were used by the fitting program to calculate the average color excess and distance modulus (indicated by the crossing lines) of each cluster. The above averages were calculated from the individual values of color excess and distance modulus of a sample of selected *single* stars, whose data points located within a previ-

ously centered *selecting error box* (see Fig. 4 and explanation below). Prior to the previous calculation, the fitting package removed probable binaries or multiple star from the sample, using a procedure based on their brighter-than-usual appearance for objects with their corresponding colors.

The coordinates of the center of the selecting error box, in the color excess - distance modulus plane, were those corresponding to the centroid of the data points contained within a pre-defined *search error box* (see Fig. 4) centered at the highest concentra-
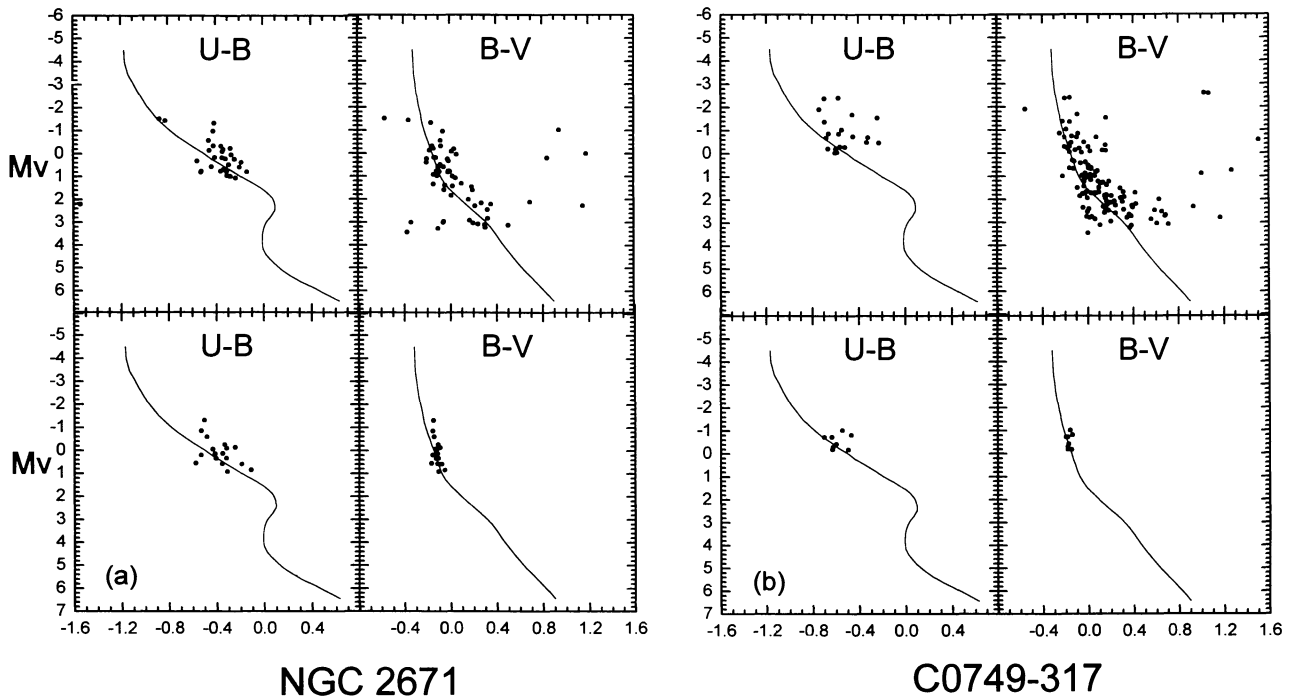
Fig. 5. Reddening free color versus absolute magnitude diagrams for NGC 2671 (*a*) and C0749–317 (*b*). The upper two panels of both (*a*) and (*b*) figures show all the stars with $U - B$ (left side) and $B - V$ (right side) data along with the corresponding ZAMS's; the absolute magnitudes were obtained by correcting the apparent magnitudes for the average absorption and distance modulus whereas the reddening free colors were computed by dereddening the observed colors using the average color excess. The lower two panels plot the reddening free colors and absolute magnitudes for only the cluster members with both $B - V$ and $U - B$ data available that were selected by the fitting program; in this case the absolute magnitudes and reddening free colors were obtained by correcting the observed magnitudes and colors for their individual absorption, distance modulus and color excess.

tion of points on this plane. In order to find the set of points with the maximum concentration, the fitting package centers a search error box on each of the points in the color excess - distance modulus diagram, and then finds out the degree of clumpiness of the rest of the points contained within the box by calculating the kurtosis of their distribution. Next, the program compares the different kurtosis values obtained for each of the sampled distributions and selects the box with the maximum value for this parameter, adopting the centroid of the data points in it as the center of the selecting error box. Once this is done, the stars within the selecting error box, centered as described, are selected as probable cluster members. The sizes of both error boxes are proportional to the expected standard deviations of the color excess and distance modulus, calculated from the photometric errors, given in the previous section, through error propagation. For more details on the reduction procedures see Pedreros (1984).

Figure 5 shows the resulting color-magnitude diagrams for the two studied clusters. The upper two

panels of both Fig. 5(*a*) and (*b*) show all the stars with observed $U - B$ (left side) and $B - V$ (right side) data along with the corresponding ZAMS's; the observed magnitudes have been corrected for the *average* absorption and distance modulus to yield the absolute magnitudes, whereas the observed colors were corrected for *average* color excess to yield the reddening free color. The lower two panels of Fig. 5(*a*) and (*b*) plot the colors and magnitudes for only the selected cluster members with both $B - V$ and $U - B$ data available; in this case the data have been corrected for their *individual* absorption, distance modulus and color excess.

The resulting average color excess and distance modulus were $E_{B-V}(B0V) = 1.04 \pm 0.02$ (s.d.) and $V_0 - M_V = 11.1 \pm 0.5$ (s.d), i.e., 1.7 (+0.4/−0.3) kpc for NGC 2671, and $E_{B-V}(B0V) = 1.26 \pm 0.04$ (s.d.) and $V_0 - M_V = 12.3 \pm 0.2$ (s.d.), i.e., 2.9 (+0.3/−0.2) kpc for C0749–317. The quoted uncertaities (s.d.'s) for the average color excesses and distance moduli were calculated, by the fitting computer package, from the scatter of the individual val-

ues of these parameters for stars within the selecting error box, thus they only account for internal errors.

An estimate of the ages of the two clusters was made by comparing their $B - V$ color-magnitude reddening-free diagrams to the theoretical isochrones by Bertelli et al. (1994) for three different metallicity values, one representing the solar chemical composition ($z = 0.0200, y = 0.28$), and the other two corresponding to a lower ($z = 0.0080, y = 0.25$) and a higher ($z = 0.0500, y = 0.352$) than solar metallicity. These latter being the two neighboring values to the solar metallicities in the isochrone grid. For these comparisons the same reddening values given above for each cluster were assumed on account that our results indicate that all of the stars in the two clusters with both $B-V$ and $U-B$ available have dereddened colors corresponding to stars earlier than A0 spectral type, which, as we know, are unaffected by the star's chemical composition. For the solar metallicity grid, the resulting ages are 8×10^7 yrs and 5×10^7 yrs for NGC 2671 and C0749–317, respectively. These values are compatible with ages obtained from the turnoff point of the $U - B$ and $B - V$ color diagrams, using Mermilliod's (1981) Age Group Parameters. As for the low and high metallicity values, we obtain ages of 9×10^7 and 6×10^7 yrs, respectively, for NGC 2671 and 6×10^7 and 5×10^7 yrs, respectively, for C0749–317. In the cases of non-solar metallicity, and for a better fit to the data, we had to slightly correct the originally adopted distance moduli. For NGC 2671 these corrections remained within the uncertainty quoted above for its distance modulus, resulting in distance moduli of 10.9 and 11.6 for the low and high metallicity values, respectively. In the case of C0749–317, the corrections amounted to twice the quoted uncertainty around the original distance modulus, giving values of 11.9 and 12.7, respectively, for its distance moduli.

At this point, in this preliminary study, it is hard to adopt a chemical composition for stars in the two clusters mainly because there are no cluster stars available around the ICCC "knee" (that is, in the $0.1 < B - V < 0.7$ color range), which is an area sensitive to chemical composition. However, in the case of C0749–317, stars 69 and 76 seem to sit very near the center of the cluster area and close to the giant branch of the high metallicity isochrones for ages 5–6 $\times 10^7$ yrs in the $B - V$ color-magnitude diagram; this would preliminary suggest a higher than solar metallicity for this cluster provided that the two mentioned stars were in fact red giant members of it.

4. CONCLUSIONS

A preliminary CCD UBV photometric study of the clusters NGC 2671 and C0749–317, located respectively, near and within the 200–260 low obscuration longitude range has been presented, obtaining reddening, distance modulus and age values (assuming solar metallicity) of $E_{B-V}(B0V) = 1.04 \pm 0.02$ (s.d.), $V_0 - M_V = 11.1 \pm 0.5$ (s.d) and 8×10^7 yrs for NGC 2671, and $E_{B-V}(B0V) = 1.26 \pm 0.04$ (s.d.), $V_0 - M_V = 12.3 \pm 0.2$ (s.d.) and 5×10^7 yrs for C0749–317. The latter cluster turned out to be the most distant and youngest of the two and deserves further study, specially because it seems to locate near the continuation of our local spiral arm feature.

REFERENCES

Bertelli, G., Bressan, A., Chiosi, C., Fagotto, F., & Nasi, E. 1994, A&AS, 106, 275
Buser, B. 1978, A&A, 62, 411
Cameron, L. M. 1985, A&A, 147, 53
FitzGerald, P. B. 1968, AJ, 73, 983
Graham, J. A. 1982, PASP, 94, 244
Heintze, J. R. N. 1973, in IAU Symp. 54, Problems of Calibration of Absolute Magnitudes and Temperatures of Stars, ed. B. Hauk & B. E. Westerlund (Dordrecht: Reidel), 231
Lucke, P. B. 1978, A&A, 64, 367
Mermilliod, J.-C. 1981, A&A, 97, 235
Pedreros, M. H. 1984, Ph.D. thesis, Univ. Toronto
Phelps, R. L., Janes, K. A., & Montgomery, K. A. 1994, AJ, 107, 1079
Ruprecht, J. 1966, Bull. Astron. Inst. Czech., 17, 34
Schmidt-Kaler, T. 1982, in Numerical Data and Functional Relationships in Science and Technology, Vol. 2, ed. K. Schaifers & H. H. Voigt (Berlin: Springer), 19
Stetson, P. B. 1987, PASP, 99, 191
Turner, D. G. 1979, PASP, 91, 642

Mario H. Pedreros: Departamento de Física, Fac. de Ciencias, Universidad de Tarapacá, Casilla 7-D, Arica, Chile (mpedrero@vitor.faci.uta.cl).